JACS
JOURNAL OF THE AMERICAN CHEMICAL SOCIETY

Communication

pubs.acs.org/JACS

A Versatile Kinetics-Controlled Coating Method To Construct Uniform Porous TiO_2 Shells for Multifunctional Core–Shell Structures

Wei Li, Jianping Yang, Zhangxiong Wu, Jinxiu Wang, Bin Li, Shanshan Feng, Yonghui Deng, Fan Zhang, and Dongyuan Zhao*

Department of Chemistry, Shanghai Key Laboratory of Molecular Catalysis and Innovative Materials, and Laboratory of Advanced Materials, Fudan University, Shanghai 200433, P. R. China

Supporting Information

ABSTRACT: The development of a simple and reproducible route to prepare uniform core@TiO_2 structures is urgent for realizing multifunctional responses and harnessing multiple interfaces for new or enhanced functionalities. Here, we report a versatile kinetics-controlled coating method to construct uniform porous TiO_2 shells for multifunctional core–shell structures. By simply controlling the kinetics of hydrolysis and condensation of tetrabutyl titanate (TBOT) in ethanol/ammonia mixtures, uniform porous TiO_2 shell core–shell structures can be prepared with variable diameter, geometry, and composition as a core (e.g., α-Fe_2O_3 ellipsoids, Fe_3O_4 spheres, SiO_2 spheres, graphene oxide nanosheets, and carbon nanospheres). This method is very simple and reproducible, yet important, which allows an easy control over the thickness of TiO_2 shells from 0 to ~25, ~45, and ~70 nm. Moreover, the TiO_2 shells possess large mesoporosities and a uniform pore size of ~2.5 nm, and can be easily crystallized into anatase phase without changing the uniform core–shell structures.

Core–shell structures, representing multiple-discrete functions related components integrated in one unit, have recently been subjected to extensive research because they promise wide applications in renewable energy, advanced biomedicine, and environmental cleanup.[1−5] The success of all these applications strongly depends on the availability of various shell frameworks with tunable composition, thickness, and structure over well-designed functional cores. Presently, a number of shell frameworks (e.g., semiconductors,[2] noble metals,[3] polymers[4]) have been developed to pursue these aims. Among those, Stöber-derived silica shells[5] are most attractive in terms of the outstanding properties of SiO_2 and in particular, the simple synthetic protocol of hydrolysis and condensation of silicon alkoxides (e.g., tetraethyl orthosilicate) in ethanol/water mixtures under alkaline conditions (e.g., ammonia)[6] Significantly, it is possible to precisely control silica shells with tunable thickness, porosity, mesostructure, and functionality.[7] Importantly, Qiao and co-workers have extended the Stöber method for preparation of uniform polymer and carbon spheres.[8] However, to date, there is rarely effective report on the preparation of other metal oxides shells, especially uniform TiO_2 shells for core–shell structures via the Stöber method.

TiO_2 is very attractive due to their fascinating features such as plentiful polymorphs, good chemical and thermal stability, excellent electronic and optical properties.[9] These features render them greatly promising in photocatalysis,[10] dye-sensitized solar cells,[11] lithium-ion batteries (LIBs),[12] and supports[13]. Therefore, it is greatly desirable to develop a simple and reproducible route to prepare core@TiO_2 structures, which is a prerequisite to realize multifunctional responses and harness multiple interfaces for new or enhanced functionalities.

Previously, great efforts have been directed toward synthesis of core@TiO_2 structures. For example, Caruso and co-workers introduced a layer-by-layer self-assembly strategy for coating TiO_2, which was realized by the surface electrostatic interactions.[14] Lou and co-workers have developed a high-temperature hydrothermal approach to synthesize a series of core@TiO_2 structures based on an interface-induced aggregation strategy.[15] In addition, several reports regarding synthesis of core@TiO_2 structures via the sol–gel method involve the use of capping agents, low temperature or mixed solvent to reduce the reactivity of titanium precursors.[16] In particular, Yin and co-workers have recently developed a two-step sol–gel process for deposition of TiO_2 on the surface of SiO_2 with the assistant of hydroxypropyl cellulose.[17] However, uniform deposition of porous TiO_2 as a thin layer to maximize the active surface is still difficult and remains a great challenge. The main reason may be the low electronegativity and the high coordination numbers of titanium, which endow its precursors with great reactivity, and thus, it is difficult to control the reaction kinetics for heterogeneous nucleation and growth of TiO_2 on desired cores.[18]

Herein, we demonstrate a versatile kinetics-controlled coating method to synthesize monodisperse core@TiO_2 shell structures. To our knowledge, this is the first report on extending the classic Stöber method to rationally control the hydrolysis and condensation of tetrabutyl titanate (TBOT) in ethanol/ammonia mixtures for constructing multifunctional core–shell structures with uniform porous TiO_2 shells. In this case, the preferential heterogeneous nucleation and growth of TiO_2 on the surface of a core (e.g., α-Fe_2O_3 ellipsoids, Fe_3O_4 spheres, SiO_2 spheres, graphene oxide nanosheets, and carbon nanospheres) can be realized by precisely controlling the reaction kinetics. This method is very simple and reproducible, yet important, which allows varying the thickness of TiO_2

Received: April 26, 2012
Published: June 29, 2012

dx.doi.org/10.1021/ja3037146 | J. Am. Chem. Soc. 2012, 134, 11864–11867

shells. In addition, the TiO_2 shells possess large mesoporosities and a uniform pore size of ~2.5 nm, and can be easily crystallized into anatase phase without changing the uniform core–shell structures. Moreover, the TiO_2 shells exhibit high performance when they are applied to lithium-ion storage and catalytic reactions.

As revealed by field emission scanning electron microscopy (FESEM) and transmission electron microcopy (TEM) images, uniform α-Fe_2O_3 ellipsoids were first synthesized with a diameter of ~100 nm and length of ~480 nm as the cores (Figure S1). Then, via a sol–gel process of hydrolysis and condensation of TBOT in ethanol/ammonia mixtures, uniform core–shell α-Fe_2O_3@TiO_2 microellipsoids can be obtained with a diameter of ~200 nm and length of ~580 nm (Figure 1a). TEM images (Figure 1b) of the microellipsoids clearly reveal the obvious core–shell structure with a porous TiO_2 shell of ~45 nm in thickness. The rough morphology reveals that the porosity results from numerous aggregated nanoparticles (Figure 1a, inset). High-magnification TEM images of the microellipsoids further confirms that individual α-Fe_2O_3 ellipsoid is uniformly coated by numerous aggregated TiO_2 nanoparticles (Figure 1c). A high-resolution TEM (HRTEM) image obviously reveals that α-Fe_2O_3 ellipsoid is well crystallized with a d-spacing of 0.25 nm matched to the d_{110} lattice,[19] and the porous TiO_2 shells are amorphous (Figure 1d and Figure S2a). The X-ray diffraction (XRD) pattern of the microellipsoids (Figure S3a) and the selected-area electron diffraction (SAED) pattern of TiO_2 shell (Figure 1c, inset) further confirm the amorphous nature of TiO_2 shells. After calcination at 500 °C in air, uniform microellipsoids are retained with a slight decrease in diameter (~190 nm) and length (~570 nm) (Figure 1e). The XRD pattern of the calcined sample (Figure S3b) exhibits the characteristic diffraction peaks, which can be well indexed to anatase TiO_2 and α-Fe_2O_3. A magnified FESEM image clearly shows that the anatase TiO_2 shells are composed of numerous aggregated nanoparticles (Figure 1e, inset). TEM observations (Figure 1f,g) further indicate that the microellipsoids possess uniform core–shell structures, where individual α-Fe_2O_3 ellipsoid is coated by self-assembled TiO_2 nanocrystals. The porous structures derived from the voids between aggregated nanocrystals can be clearly elucidated. The corresponding SAED pattern of the shells (Figure 1g, inset) also reveals the polycrystalline feature of anatase TiO_2. The mean shell thickness is estimated to be ~40 nm (Figure 1g). In contrast, the slight shrinkage of TiO_2 shells after calcination may be attributed to the desorbed water and the condensation of TiO_2 networks at a high temperature as demonstrated by the thermogravimetric analysis (TGA, Figure S4). HRTEM images (Figure 1h and Figure S2b) show that the TiO_2 nanoparticles are well crystallized with a size of ~5 nm and a d-spacing of 0.35 nm, well-matched to the d_{101} of anatase TiO_2,[20] and exhibit highly mesoporous structures.

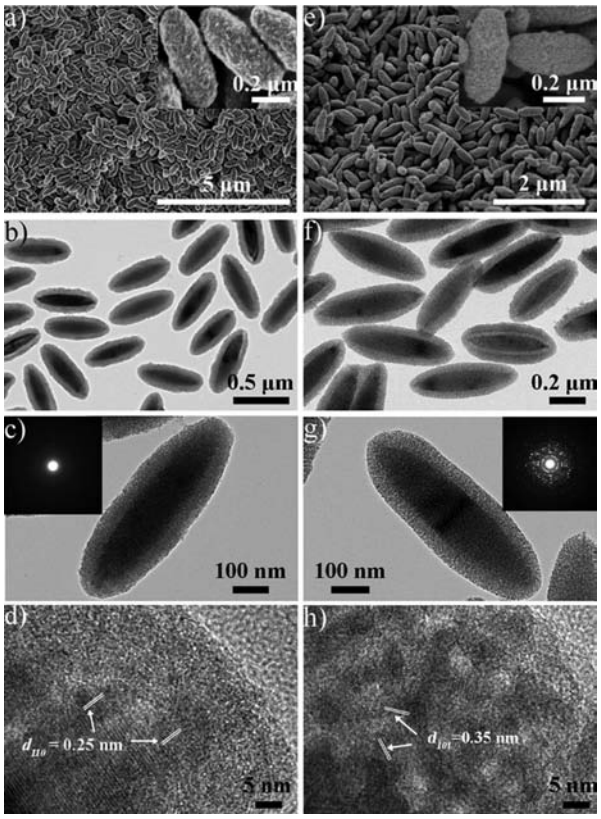

Figure 1. The core–shell α-Fe_2O_3@TiO_2 microellipsoids prepared by the kinetics-controlled coating method: (a) FESEM images; (b,c) TEM images and (d) HRTEM images before calcinations. (e) FESEM images; (f,g) TEM images and HRTEM images after calcinations at 500 °C in air. The insets in (a) and (e) are the corresponding magnified FESEM images, showing the nanoparticles-aggregated structures. The insets in (c) and (g) are the corresponding SAED patterns taken from the shell domain, revealing the polycrystalline feature of anatase TiO_2.

N_2 sorption isotherms (Figure S5A) of the core–shell α-Fe_2O_3@TiO_2 microellipsoids before and after calcination both show typical type IV curves with distinct hysteresis loops close to H1 type. The Brunauer–Emmett–Teller (BET) surface area and pore volume of the as-prepared microellipsoids are calculated to be as high as 404 m^2/g and 0.35 cm^3/g, respectively, further revealing the highly porous shell structures. After calcination at 500 °C in air, the BET surface area and pore volume are greatly decreased to 105 m^2/g and 0.16 cm^3/g, respectively, but still high. This results from the densification of TiO_2 networks and the growth of nanocrystals. The corresponding pore size distribution curves (Figure S5B) derived from the adsorption branches of the isotherms by using the Barrett–Joyner–Halenda (BJH) method clearly show a slightly larger pore size of ~4.3 nm than that (~2.5 nm) of the as-prepared sample, further illustrating that small amorphous nanoparticles are aggregated, and grow into large anatase nanocrystals. Such large mesoporosities derived from the uniform TiO_2 nanoparticles, in association with the very thin layer of TiO_2, are expected to show high performances when they are applied to lithium-ion storage and catalytic reactions (see Figures S6 and S7).[21]

The effect of ammonia content is analyzed to gain insight into the formation mechanisms of the uniform porous TiO_2 shells. When a small fraction of ammonia is added to the system (<0.2 vol %), FESEM images show that no obvious TiO_2 nanoparticles are formed on the surface of α-Fe_2O_3 ellipsoids (Figure S8a,b). Once the content of 0.25 vol % ammonia is reached, uniform TiO_2 shells (~25 nm in thickness) can be constructed on the surface of α-Fe_2O_3 ellipsoids (Figures S8c and S9a). After removing the core–shell α-Fe_2O_3@TiO_2 microellipsoids from the mixtures, a clear solution can be obtained (Figure S10a), indicating that heterogeneous nucleation and growth of TiO_2 on the surface of α-Fe_2O_3

dx.doi.org/10.1021/ja3037146 | J. Am. Chem. Soc. 2012, 134, 11864–11867

ellipsoids preferentially occur over homogeneous ones. As ammonia content increases to 0.4 vol %, the thickness of TiO_2 shells increases to ~70 nm (Figures S8d and S9b), and a milky white suspension is observed after removing the microellipsoids (Figure S10b). It reveals that isolated TiO_2 nanoparticles are formed in the solution (Figure S8f). However, under the same ammonia content of 0.4 vol %, just shortening the reaction time to 12 h, a clear solution is obtained after removing the microellipsoids (Figure S10c), and yet the thickness of TiO_2 shells (~70 nm) is not obviously changed (Figure S8e). These observations illustrate that further growth and polymerization of titanium oligomers cannot occur on the surface of the microellipsoids when the thickness of TiO_2 shells reaches ~70 nm, but homogeneous nucleation and growth can take place in the solution with time; thus, isolated TiO_2 nanoparticles are formed. When 1.0 vol % water mixed with 0.4 vol % ammonia is added into the synthetic system, large irregular nanoparticles are observed (Figure S8g), which indicates that excess amount of catalyst make the hydrolysis and condensation of TBOT so rapid that heterogeneous and homogeneous nucleation and growth occur simultaneously; thus, aggregated structures are formed. These results clearly demonstrate that ammonia content plays an important role in controlling the reaction kinetics to construct uniform core−shell α-Fe_2O_3@TiO_2 microellipsoids.

On the basis of the above observations, we propose a kinetics-controlled coating process for uniformly coating TiO_2 on the surface of α-Fe_2O_3 ellipsoids. The sol−gel process of a titanium alkoxide to form a polymerized TiO_2 networks consists of hydrolysis and condensation steps as depicted in Figure 2; consequently, the kinetics of hydrolysis and condensation over TBOT are mainly controlled by the concentration of ammonia while maintaining other reaction parameters.[18] Figure 2b schematically illustrates the four distinct modes observed for nucleation and growth of TiO_2 on the surface of α-Fe_2O_3 ellipsoids under different ammonia content. When adding a small fraction of ammonia into the system (Mode 1), the hydrolysis and condensation rate of TBOT is very slow, resulting in a low concentration of titanium oligomers (C_{to}). Because the C_{to} is lower than the critical concentration for heterogeneous nucleation (C_{he}), no TiO_2 nanoparticles are formed on the surface of α-Fe_2O_3 ellipsoids. Upon slightly increasing the content of ammonia (Mode 2), the hydrolysis and condensation of TBOT can be promoted, thus leading to a quick increasing of titanium oligomers. When the C_{to} reaches a level higher than the C_{he}, a significant heterogeneous nucleation of TiO_2 takes place on the surface of α-Fe_2O_3 ellipsoids. The appearance of TiO_2 nuclei partially relieves some titanium oligomers, however, which is still higher than the supersaturated concentration (C_{sat}), because of the balance between the production by hydrolysis and condensation and the consumption by diffusion to the nuclear sinks.[18,22] Therefore, the process of growth of TiO_2 nuclei to form TiO_2 networks can proceed through diffusion and polymerization of titanium oligomers to the TiO_2 nuclei. Finally, uniform TiO_2 shells are formed. With a high content of ammonia (Mode 3), the reaction kinetics is greatly enhanced; thus, the C_{to} is initially increased extraordinary high. As a result, TiO_2 nuclei are formed in a short time. In this case, the plentiful supplies of titanium oligomers make TiO_2 shells rapidly grow in thickness, but simultaneously, the growth rate becomes slow with time as a result of the mass transfer and the diffusion of reactive species to large particles is much slower than that of small ones.[22]

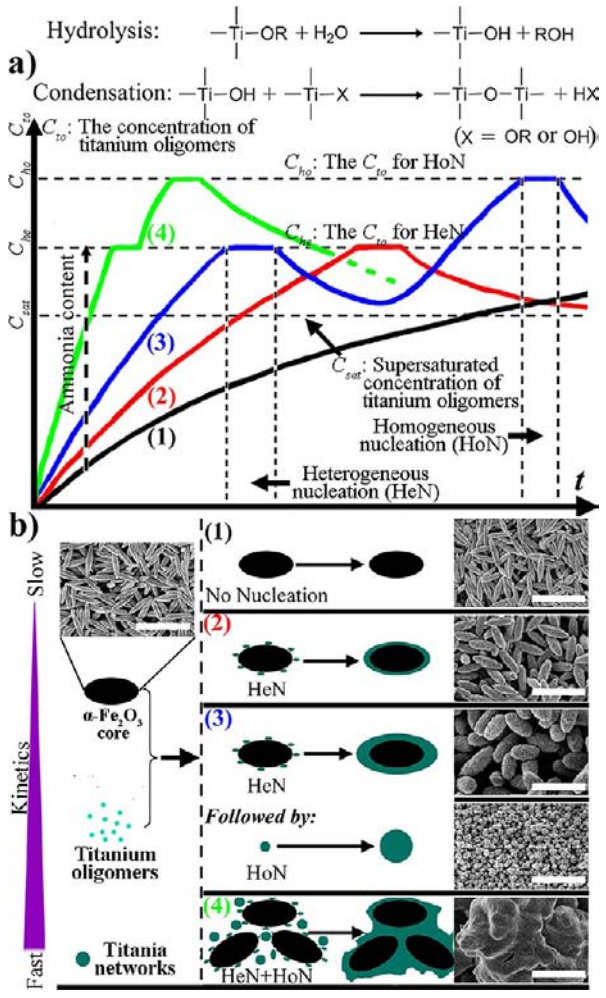

Figure 2. (a) Schematic illustration of the hydrolysis and condensation process of titanium alkoxides for preparing polymerized TiO_2 networks. (b) Schematic representation of nucleation and growth of TiO_2 on the surface of α-Fe_2O_3 cores via the kinetics-controlled coating method. The plot shows four distinct modes of the time-dependant concentration of titanium oligomers (C_{to}) under different ammonia content, the corresponding representation (left) of nucleation and growth process of TiO_2 on the surface of α-Fe_2O_3 cores in each mode and the SEM images (right) of resulted α-Fe_2O_3/TiO_2 composites are also illustrated. The scale bar of all SEM images is 1 μm.

When a maximum thickness of ~70 nm is obtained, the growth of TiO_2 shells is suppressed due to the size effect.[22] Therefore, with further hydrolysis and condensation of TBOT, the C_{ho} can eventually be reached so the isolated TiO_2 nanoparticles are formed. If the initial contents of water and ammonia are too high (Mode 4), the reaction kinetics becomes so fast that the C_{to} can continually exceed the C_{ho} where even the heterogeneous nucleation occurs. As a result, a continual cascading of nuclei in addition to growth ensues. Obviously, then, large nanoparticles are formed and aggregated. Consequently, by controlling the reaction kinetics, homogeneous nucleation and growth of TiO_2 can be avoided so that uniform core−shell α-Fe_2O_3@TiO_2 structures can proceed, and importantly, the thickness of TiO_2 shell can be tailored by adjusting the initial ammonia content.

We further demonstrate that Fe_3O_4 spheres, Stöber-derived silica spheres, as well as graphene oxide (GO) nanosheets

dx.doi.org/10.1021/ja3037146 | J. Am. Chem. Soc. 2012, 134, 11864−11867

(Figure S11) can be uniformly coated by porous TiO_2 shells via the kinetics-controlled coating method; all the samples obviously show the monodisperse core−shell structures (Figure 3). In addition, uniform porous TiO_2 shells can also be

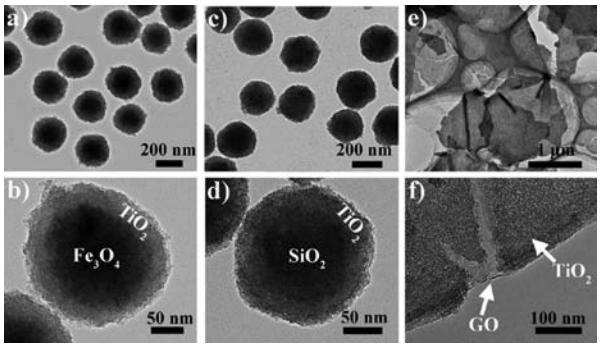

Figure 3. TEM images of the uniform porous TiO_2 shell core−shell structures prepared by the kinetics-controlled coating method: (a,b) Fe_3O_4@TiO_2 spheres, (c,d) SiO_2@TiO_2 spheres and (e,f) graphene oxides (GO)@TiO_2 nanosheets. The white labels obviously show the corresponding cores and the TiO_2 shells domain.

constructed on the surface of carbon nanospheres (Figure S12). Silica is well-known for its versatility in coating many nanostructures to form core−shell structures.[23] Therefore, we have also demonstrated that uniform porous TiO_2 shells can be constructed with a silica interlayer. For example, monodisperse sandwich-like core−shell structures can be obtained with Fe_3O_4 or $NaYF_4$:Yb,Er nanoparticles as the inner core, silica as the interlayer, and uniform porous TiO_2 as the outer shells (Figure S13). These observations illustrate that uniform porous TiO_2 shells can be coated on surface of various cores via the kinetics-controlled coating method independent of core diameter, geometry, and composition.

In summary, we have demonstrated a versatile kinetics-controlled coating method to construct uniform porous TiO_2 shells for multifunctional core−shell structures such as α-Fe_2O_3@TiO_2 microellipsoids, Fe_3O_4@TiO_2 spheres, SiO_2@TiO_2 spheres, GO@TiO_2 nanosheets, and carbon@TiO_2 spheres. The preferential heterogeneous nucleation and growth of TiO_2 on the core surface can be realized by precisely controlling the kinetics of hydrolysis and condensation of TBOT in ethanol/ammonia mixtures. Noteworthy, the thickness of the TiO_2 shells can be varied from 0 to ∼25, ∼45 and ∼70 nm by adjusting the ammonia content, and importantly, they possess large mesoporosities and a uniform pore size of ∼2.5 nm. In addition, the amorphous TiO_2 can easily transform to anatase phase without changing the uniform core−shell structures. We believe that such a demonstration presents a new powerful approach toward preparing high-performance and multifunctional core@TiO_2 structures and, more importantly, provides insight into the design of advanced core−shell structures.

■ ASSOCIATED CONTENT

Supporting Information

Detailed experimental procedures, characterization methods, SEM images, XRD data, N_2 sorption results, TEM images and LIBs performance measurements. This material is available free of charge via the Internet at http://pubs.acs.org.

■ AUTHOR INFORMATION

Corresponding Author

dyzhao@fudan.edu.cn

Notes

The authors declare no competing financial interest.

■ ACKNOWLEDGMENTS

This work was supported by the NSF of China (20890123), the State Key Basic Research Program of the PRC (2009AA033701and 2009CB930400), Science and Technology Commission of Shanghai Municipality (08DZ2270500), and Shanghai Leading Academic Discipline Project (B108).

■ REFERENCES

(1) Chaudhuri, R. G.; Paria, S. *Chem. Rev.* **2012**, *112*, 2373.
(2) (a) Tang, J. Y.; Huo, Z. Y.; Brittman, S.; Gao, H. W.; Yang, P. D. *Nat. Nanotechnol.* **2011**, *6*, 568. (b) Li, W.; Deng, Y.; Wu, Z.; Qian, X.; Yang, J.; Wang, Y.; Gu, D.; Zhang, F.; Tu, B.; Zhao, D. *J. Am. Chem. Soc.* **2011**, *133*, 15830. (c) Xiong, Z. G.; Zhao, X. S. *J. Am. Chem. Soc.* **2012**, *134*, 5754.
(3) Feng, Y.; He, J.; Wang, H.; Tay, Y.; Sun, H.; Zhu, L.; Chen, H. Y. *J. Am. Chem. Soc.* **2012**, *134*, 2004.
(4) Sindoro, M.; Feng, Y.; Xing, S.; Li, H.; Xu, J.; Hu, H.; Liu, C.; Wang, Y.; Zhang, H.; Shen, Z.; Chen, H. Y. *Angew. Chem., Int. Ed.* **2011**, *50*, 9898.
(5) (a) Joo, S. H.; Park, J. Y.; Tsung, C. K.; Yamada, Y.; Yang, P. D.; Somorjai, G. A. *Nat. Mater.* **2009**, *8*, 126. (b) Kim, J.; Kim, H. S.; Lee, N.; Kim, T.; Kim, H.; Yu, T.; Song, I. C.; Moon, W. K.; Hyeon, T. *Angew. Chem., Int. Ed.* **2008**, *47*, 8438. (c) Ge, J. P.; Hu, Y. X.; Yin, Y. D. *Angew. Chem., Int. Ed.* **2007**, *46*, 7428.
(6) Stöber, W.; Fink, A.; Bohn, E. *J. Colloid Interface Sci.* **1968**, *26*, 62.
(7) (a) Zhang, L.; Qiao, S. Z.; Jin, Y. G.; Chen, Z. G.; Gu, H. C.; Lu, G. Q. *Adv. Mater.* **2008**, *20*, 805. (b) Piao, Y. Z.; Burns, A.; Kim, J.; Wiesner, U.; Hyeon, T. *Adv. Funct. Mater.* **2008**, *18*, 3745. (c) Ge, J. P.; Yin, Y. D. *Adv. Mater.* **2008**, *20*, 3485.
(8) Liu, J.; Qiao, S. Z.; Liu, H.; Chen, J.; Orpe, A.; Zhao, D.; Lu, G. Q. *Angew. Chem., Int. Ed.* **2011**, *50*, 5947.
(9) Chen, X.; Mao, S. S. *Chem. Rev.* **2007**, *107*, 2891.
(10) Liu, S.; Yu, J.; Jaroniec, M. *J. Am. Chem. Soc.* **2010**, *132*, 11914.
(11) Feng, X. J.; Zhu, K.; Frank, A. J.; Grimes, C. A.; Mallouk, T. E. *Angew. Chem., Int. Ed.* **2012**, *51*, 2727.
(12) Wang, Z. Y.; Zhou, L.; Lou, X. W. *Adv. Mater.* **2012**, *24*, 1903.
(13) Lee, I.; Joo, J. B.; Yin, Y. D.; Zaera, F. *Angew. Chem., Int. Ed.* **2011**, *50*, 10208.
(14) Caruso, F.; Shi, X.; Caruso, R. A.; Susha, A. *Adv. Mater.* **2001**, *13*, 740.
(15) (a) Lou, X. W.; Archer, L. A. *Adv. Mater.* **2008**, *20*, 1853. (b) Chen, J. S.; Chen, C. P.; Liu, J.; Xu, R.; Qiao, S. Z.; Lou, X. W. *Chem. Commun.* **2011**, *47*, 2631.
(16) (a) Sakai, H.; Kanda, T.; Shibata, H.; Ohkubo, T.; Abe, M. *J. Am. Chem. Soc.* **2006**, *128*, 49447. (b) Demirörs, A. F.; van Blaaderen, A.; Imhof, A. *Langmuir* **2010**, *26*, 929.
(17) Ye, M. M.; Zhang, Q.; Hu, Y. X.; Ge, J. P.; Lu, Z. D.; He, L.; Chen, Z. L.; Yin, Y. D. *Chem.−Eur. J.* **2010**, *16*, 6243.
(18) (a) Livage, J.; Henry, M.; Sanchez, C. *Prog. Solid State Chem.* **1988**, *18*, 259. (b) Barringer, E.; Bowen, H. *Langmuir* **1985**, *1*, 414.
(19) Chen, J. S.; Zhu, T.; Li, C. M.; Lou, X. W. *Angew. Chem., Int. Ed.* **2011**, *50*, 650.
(20) Ma, X. Y.; Chen, Z. G.; Hartono, S. B.; Jiang, H. B.; Zou, J.; Qiao, S. Z.; Yang, H. G. *Chem. Commun.* **2010**, *46*, 6608.
(21) (a) Guo, Y. G.; Hu, J. S.; Wan, L. J. *Adv. Mater.* **2008**, *20*, 2878. (b) Sushko, M.; Rosso, K.; Liu, J. *J. Phys. Chem. Lett.* **2010**, *1*, 1967.
(22) (a) Lamer, V. K.; Dinegar, R. H. *J. Am. Chem. Soc.* **1950**, *72*, 4847. (b) Bogush, G.; Zukoski, C. *J. Colloid Interface Sci.* **1991**, *142*, 1.
(23) Lu, Z. D.; Gao, C. B.; Zhang, Q.; Chi, M. F.; Howe, J. Y.; Yin, Y. D. *Nano Lett.* **2011**, *11*, 3404.